Feedback Cooling of a One-Electron Oscillator

B. D'Urso, B. Odom, and G. Gabrielse

Department of Physics, Harvard University, Cambridge, Massachusetts 02138

(Received 4 September 2002; published 28 January 2003)

A one-electron oscillator is cooled from 5.2 K to 850 mK using electronic feedback. Novel quantum jump thermometry reveals a Boltzmann distribution of oscillator energies and directly measures the corresponding temperature. The ratio of electron temperature and damping rate (also directly measured) is observed to be a fluctuation-dissipation invariant, independent of feedback gain, as predicted for noiseless feedback. The sharply reduced linewidth that results from feedback cooling illustrates the likely importance for improved fundamental measurements and symmetry tests.

DOI: 10.1103/PhysRevLett.90.043001 PACS numbers: 32.80.Pj, 42.50.Lc, 42.50.Vk

At a time when the importance of feedback for reducing amplifier noise was already recognized [1], Kittel described the general theory and limits of "noiseless" feedback damping [2]. Feedback damping has been applied in subsequent decades to a variety of oscillatory systems including an electrometer [3], a torsion balance [4], a mechanical gravity gradiometer [5], a laboratory rotor [6], a vibration mode of an optical mirror [7], and to the stochastic cooling of particle beams [8]. The possible application of Kittel's noiseless feedback to trapped particles was mentioned [9], as was the relevance of the limitations he discussed [10] to proposed stochastic cooling of trapped antiprotons [11]. Using feedback to improve measurements is an active area of current research [12].

This Letter describes the feedback cooling of the simplest of oscillators—one with demonstrated potential for fundamental measurements. A one-electron oscillator is cooled from 5.2 to 0.85 K. A unique feature is that this classical oscillator's temperature and damping rate are both determined absolutely by measuring frequencies. A novel feature is that quantum jump thermometry (utilizing quantum electron cyclotron motion orthogonal to the cooled classical oscillation) directly displays the Boltzmann distribution of oscillator energies [13]. The measurements reveal cooling to an ideal, noiseless feedback limit that is characterized by a fluctuation-dissipation invariant. Noise added by the active feedback electronics limits the lowest temperature attained.

The observed narrowing of an electron's cyclotron resonance line, with similar narrowing of the "anomaly" resonance [14] at the difference of its spin and cyclotron frequencies, will allow higher precision measurements of these frequencies and more precise systematic studies. The higher accuracy determination of these frequencies expected as a result could enable better measurements of the magnetic moments of the electron and positron, an improved determination of the fine structure constant, an improved *CPT* test with leptons, and a better measurement of the proton-to-electron mass ratio.

The oscillation cooled with feedback is that of a single electron along the central symmetry axis ($\hat{z}$) of a cylindrical Penning trap [15,16] (Fig. 1). The trap electrodes are biased so the electron oscillates in a harmonic potential well ($\sim z^2$) with frequency $\nu_z = 64.787$ MHz. The z^4 well distortion is tuned out by adjusting the potential on small, orthogonalized compensation electrodes [15].

We treat the one-electron oscillator as a charge attached to a massless spring, focusing upon potentials and currents that oscillate near ν_z, while ignoring the additional static trapping potentials always applied to the trap. Oscillatory potentials applied to either of the two end-plate electrodes (Fig. 2) drive the electron oscillator. The electron motion, in turn, induces a current I to flow through R, a resistance due to unavoidable loss in an attached amplifier and inductor. The inductor (in parallel to R but not shown) tunes out trap capacitance (e.g., between the plates).

With no feedback [Fig. 2(a)], the induced current I removes energy from the electron oscillator at the familiar rate I^2R, with the result that the damping rate $\Gamma \propto R$. The proportionality constant depends upon the electron charge, the electron mass, and the geometry of the trap [14]. Measurements to be discussed show that the electron oscillator is weakly damped (i.e., $\Gamma/2\pi \ll \nu_z$) with $\Gamma/2\pi = 8.4$ Hz.

The random thermal fluctuations of electrons within R, in thermal equilibrium at temperature T, produce a fluctuating Johnson-Nyquist noise potential [17,18] V_n. This frequency independent white noise, with

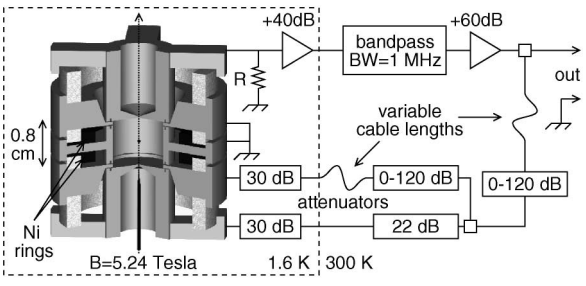

FIG. 1. Representation of trap and high frequency electronics used for feedback cooling. Static potentials applied to suspend the electron at the trap center are not shown.

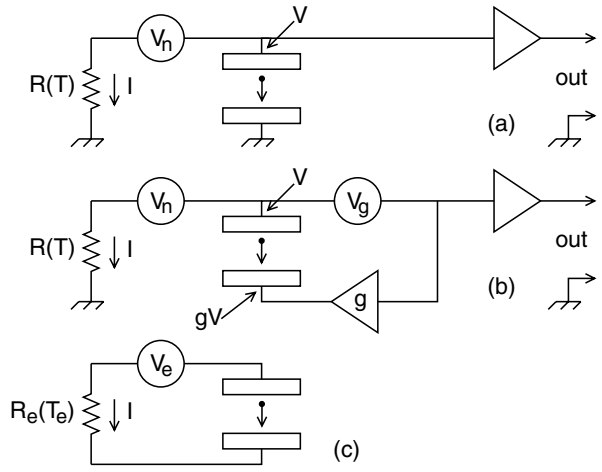

FIG. 2. Conceptual circuit without (a) and with (b) feedback. For ideal noiseless feedback, $V_g = 0$. For the electron, circuits (b) and (c) are equivalent.

$$\overline{V_n^2} = 4kTR\Delta\nu \tag{1}$$

in a frequency bandwidth $\Delta\nu$, drives the electron. This noise and the induced current both contribute to the voltage on the upper plate, $V = V_n + IR$. A sensitive HEMT (high electron mobility transistor) amplifier [19] amplifies V so it can be detected.

The measured power spectrum for V [Fig. 3(a)] has a constant baseline due to the Johnson noise. The current induced by the noise-driven electron produces a notch in this flat spectrum at ν_z; the angular frequency width of this notch is the damping rate Γ. The notch is most easily understood if the oscillating charge is represented as a familiar electrical oscillator, an inductor ℓ, and a capacitor c in series, connected between the plates. On resonance at ν_z the electron acts as an electrical short between the plates since the reactances of the ℓ and c cancel. The notch has the characteristic Lorentzian shape of a damped harmonic oscillator. The observed noise cancellation is not perfect [i.e., the dip does not go perfectly to zero power in Fig. 3(a)] because of amplifier noise, trap potentials that are not perfectly stable, and residual trap anharmonicity.

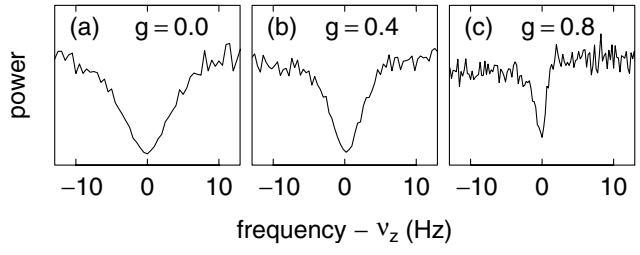

FIG. 3. Oscillator damping rate Γ_e (the width of the notch in the white Johnson noise) without feedback (a) and when decreased using feedback (b) and (c).

When the amplifier is on, as it must be for feedback to be applied, measurements to be discussed show that R is at a temperature of 5.2 K. This is higher than the 1.6 K of the trap apparatus (maintained by thermal contact to a pumped ^{4}He system), despite the minimal 420 μW power dissipation of the current-starved HEMT, and heroic efforts to thermally anchor the HEMT at 1.6 K.

Feedback is applied as shown conceptually in Fig. 2(b). The fluctuating upper plate voltage V is fed back to the lower plate with feedback gain, g. A more complete representation (Fig. 1) shows amplifiers, attenuators, and variable cable lengths used to adjust the feedback phases. Correctly phased feedback to two electrodes, rather than just to the bottom plate in the conceptual Fig. 2(b), applies feedback to the electron while canceling feedback to the amplifier. Feedback to the amplifier would modify its properties [1], perhaps improving particle detection in some situations [20], but would complicate the relationship between feedback gain, electron temperature, and electron damping.

For the electron, the effect of feedback is equivalent to the circuit in Fig. 2(c), with R_e and T_e chosen to make the motion-induced potential and the fluctuation potential across the plates the same as for Fig. 2(b).

To determine R_e (and hence the damping rate $\Gamma_e \propto R_e$) we insist that electron motion induces the same potential difference across the plates. Equating $IR - gIR$ for Fig. 2(b) with IR_e for Fig. 2(c) yields $R_e = (1 - g)R$, and an electron damping rate

$$\Gamma_e = (1 - g)\Gamma. \tag{2}$$

When $g = 0$, we recover the damping rate Γ for no feedback. When $g = 1$, the electron oscillator is undamped.

To determine the effective temperature T_e we insist that the electron see the same noise fluctuations across the plates in Figs. 2(b) and 2(c). Equating $V_n - gV_n$ for Fig. 2(b) with V_e for Fig. 2(c) yields

$$T_e = (1 - g)T. \tag{3}$$

We recover the resistor temperature T when there is no feedback ($g = 0$). The temperature decreases as the feedback gain is increased. We shall see that noise added in the feedback process prevents attaining 0 K as $g \to 1$.

The fluctuations (characterized by a temperature) and the dissipation (characterized by a damping rate) are related for ideal, noiseless feedback by a fluctuation-dissipation invariant [2],

$$T_e/\Gamma_e = T/\Gamma. \tag{4}$$

Noiseless feedback with gain $g < 0$ increases the damping rate but at the expense of also increasing the temperature and fluctuations. Noiseless feedback cooling, with $0 < g < 1$, decreases the temperature, but at the expense of reducing the damping rate. The advantage of a reduced T_e is to reduce deleterious effects of axial

fluctuations upon other electron motions, as we will illustrate with a reduced cyclotron linewidth.

Real feedback amplifiers add fluctuations V_g that increase T_e above the the ideal Eqs. (3) and (4), and reduce the depth of the observed Lorentzian noise notch. Equating the fluctuations across the plates for Figs. 2(b) and 2(c) yields

$$T_e = T\left[1 - g + \frac{g^2}{1-g}\frac{T_g}{T}\right]. \quad (5)$$

T_g is a feedback "noise temperature" such that $\overline{V_g^2}/\overline{V_n^2} = T_g/T$. The relative depth of the Lorentzian notch in the observed noise power,

$$F = 1 - (1-g)^{-2}(1 + T/T_g)^{-1}, \quad (6)$$

is the ratio of this noise power on and off resonance.

T_e initially drops linearly with g increasing from zero as in the ideal case [Eq. (3)]. [An example is the function fit to measured temperatures in Fig. 5(a), discussed later.] T_e then rises rapidly as $g \to 1$, the limit of an undamped oscillator driven by feedback noise.

The lowest temperature $T_e(\min) \approx 2\sqrt{T_g T}$, for $T_g \ll T$, is at an optimal feedback gain $g \approx 1 - \sqrt{(T_g/T)}$, and our amplifier has $T_g \approx 40$ mK. Meanwhile, the deep notch ($F \approx 1$ for $g = 0$) goes to essentially no notch at all ($F \approx 0$) at the gain that minimizes T_e. Damping remains but we cannot measure its rate by this method.

The temperature T_e of the effective damping resistance is important because the electron axial oscillation comes into thermal equilibrium at T_e. Averaged over many axial damping times Γ^{-1}, the probability that the oscillator has energy between E_z and $E_z + dE_z$ goes as the Boltzmann factor, e^{-E_z/kT_e}.

Remarkably, we can directly measure this Boltzmann distribution, and hence T_e, using quantum jump thermometry. The quantum jumps [13] are between the ground and first excited states of the electron's cyclotron motion in a 5.24 Tesla magnetic field directed along the electron's axial oscillation (Fig. 1). Compared to the rapid 146.7 GHz cyclotron motion the axial motion is adiabatic. It is unaffected by a single quantum cyclotron excitation except for the tiny shift of ν_z [Eq. (8)] that we discuss next. The cyclotron damping lifetime is extended to 15 s (from 0.1 s for free space) using a trap cavity that inhibits spontaneous emission [13].

The coupling of cyclotron and axial motion comes from the small "magnetic bottle" gradient [14] from two small nickel rings (Fig. 1). The electron sees a magnetic field that increases slightly as z^2 as it moves away from the center of the trap in its axial oscillation. This coupling shifts the cyclotron frequency by a measured [13] $\delta = 12$ Hz for every quantum of axial excitation,

$$\Delta\nu_c = \delta(E_z/h\nu_z). \quad (7)$$

The axial frequency shifts by the same amount,

$$\Delta\nu_z = \delta(E_c/h\nu_c), \quad (8)$$

for every quantum of cyclotron excitation. Both tiny shifts are used for the quantum jump thermometry.

A Boltzmann distribution of axial energies, owing to Eq. (7), makes an associated distribution of cyclotron frequencies, given that the axial damping time is longer than the time associated with the noise fluctuations of the axial frequency [14]. A cyclotron driving force at frequency ν excites a quantum jump between the ground and first excited cyclotron states with a probability

$$P(\nu) \sim \begin{cases} 0, & \nu < \nu_c, \\ e^{-(\nu_z/\delta)[h(\nu-\nu_c)/kTe]}, & \nu > \nu_c, \end{cases} \quad (9)$$

provided that the jumps happen more rapidly than the one per hour stimulated by black body photons in the 1.6 K trap cavity.

To determine whether a quantum jump has taken place we look for the corresponding axial frequency shift [Eq. (8)]. We do not simply observe the center frequency of a noise dip (Fig. 3), though this would likely suffice. Instead, before a cyclotron excitation decays (in typically 15 s), we observe the electron's response to a strong axial drive for the 1 s needed to measure $\Delta\nu_z$ and determine the cyclotron state.

The measurement cycle starts with 0.5 s of magnetron sideband cooling [14] to keep the electron near the center axis of the trap. Feedback cooling is then applied for 6 s, with the cyclotron drive at ν turned on for the last two of these seconds. The axial drive to determine $\Delta\nu_z$ and the cyclotron state is applied next, along with more magnetron cooling. The cyclotron state is read out once each second until the ground state is observed for 2 s. The cycle then repeats.

The measured cyclotron line shapes (Fig. 4) narrow significantly as the feedback gain increases. Each shows

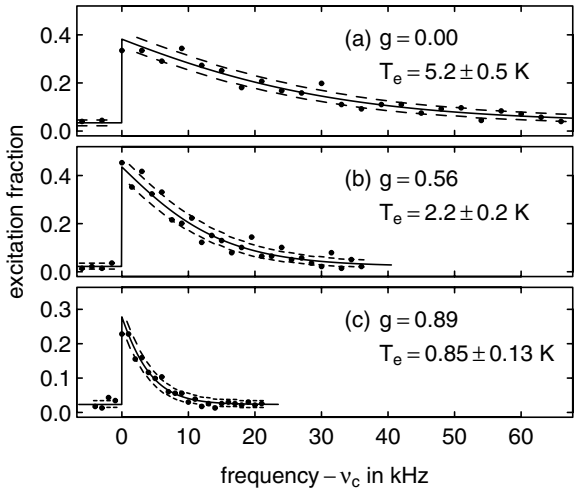

FIG. 4. Cyclotron resonances show Boltzmann distributions of axial energies that decrease in width as the feedback gain g is increased. Dashed lines bound the 68% confidence area.

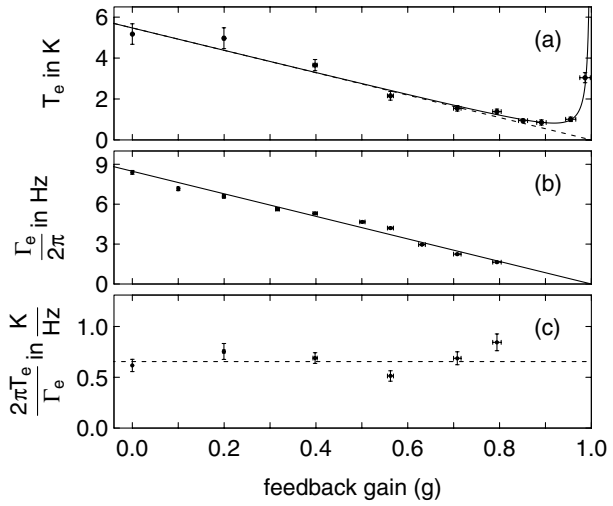

FIG. 5. Axial temperature (a), damping rate (b), and the fluctuation-dissipation invariant (c) as a function of feedback gain. The dotted line in (c) is the weighted average.

the characteristic Boltzmann distribution that signifies thermal equilibrium. Each is fit to Eq. (9) to determine the equilibrium axial temperature, T_e. The lowest observed $T_e = 850$ mK [Fig. 4(c)] is a substantial reduction of the 5.2 K realized without feedback.

The measured axial temperature [Fig. 5(a)] decreases linearly as g increases from 0, as predicted in Eqs. (3) and (5). There is a good fit to Eq. (5), including the rapid increase for $g \rightarrow 1$ which corresponds to a nearly undamped system being driven by the noise added in the feedback signal. It is difficult to fix g accurately enough to measure points on this rapid rise.

The damping rate Γ_e, the width of a noise dip (e.g., Fig. 3), is measured directly [Fig. 5(b)]. The damping rate decreases linearly with increasing g as predicted in Eq. (2). The vanishing dip width and the instabilities mentioned earlier keep us from measuring Γ near $g = 1$.

Because we directly measure T_e (characterizing fluctuations) and Γ_e (characterizing dissipation) we can compare their ratio [Fig. 5(c)] to the fluctuation-dissipation invariant that pertains for noiseless feedback [Eq. (4)]. The measured ratio is invariant and is at the ideal limit, though we expect that it would rise above the ideal limit if we could measure it for feedback gains closer to unity.

In conclusion, feedback cooling to the noiseless limit is demonstrated with the simplest of oscillators. Characterization of the cooling of a one-electron oscillator is direct and complete because both fluctuations and dissipation are directly and absolutely determined by frequency measurements. In addition, sharply narrowed cyclotron line shapes present the possibility of much more accurate measurements of the electron cyclotron frequency, with similar line narrowing and accuracy improvement expected for the electron anomaly resonance [14]. Better measurements of these frequencies for a single trapped electron and positron opens the way to better measurements of their magnetic moments, a more accurate value of the fine structure constant, a more precise test of *CPT* invariance for leptons, and an improved proton-to-electron mass ratio.

We are grateful for wonderful electronics support from J. MacArthur, and for lab assistance from A. Steinert, O. Elliott, and R. van Handel. This work was supported by the NSF, the ONR, and the AFOSR. B. D. was also supported by the Fannie and John Hertz Foundation.

[1] M. Strutt and A. Van der Ziel, Physica **9**, 513 (1942).
[2] C. Kittel, *Elementary Statistical Physics* (Wiley, New York, 1958), pp. 141–156.
[3] J. Milatz, J.V. Zolingen, and B.V. Iperen, Physica **19**, 195 (1953).
[4] P. Roll, R. Krotkov, and R. Dicke, Ann. Phys. (N.Y.) **26**, 442 (1964).
[5] R. Forward, J. Appl. Phys. **50**, 1 (1979).
[6] B. Bernard and R. Ritter, J. Appl. Phys. **64**, 2833 (1988).
[7] P. F. Cohadon, A. Heidmann, and M. Pinard, Phys. Rev. Lett. **83**, 3174 (1999).
[8] S. van der Meer, Rev. Mod. Phys. **57**, 689 (1985).
[9] H. Dehmelt, W. Nagourney, and J. Sandberg, Proc. Natl. Acad. Sci. U.S.A. **83**, 5761 (1986).
[10] S. Rolston and G. Gabrielse, Hyperfine Interact. **44**, 233 (1988).
[11] N. Beverini, V. Lagomarsino, G. Manuzio, F. Scuri, G. Testera, and G. Torelli, Phys. Rev. A **38**, 107 (1988).
[12] J. Courty, F. Grassia, and S. Reynaud, quant-ph/0110021.
[13] S. Peil and G. Gabrielse, Phys. Rev. Lett. **83**, 1287 (1999).
[14] L. S. Brown and G. Gabrielse, Rev. Mod. Phys. **58**, 233 (1986).
[15] G. Gabrielse and F. C. MacKintosh, Int. J. Mass Spectrom. Ion Process. **57**, 1 (1984).
[16] J. N. Tan and G. Gabrielse, Appl. Phys. Lett. **55**, 2144 (1989).
[17] J. Johnson, Phys. Rev. **32**, 97 (1928).
[18] H. Nyquist, Phys. Rev. **32**, 110 (1928).
[19] To be published.
[20] S. Rainville, M. Bradley, J. Porto, J. Thompson, and D. Pritchard, Hyperfine Interact. **132**, 177 (2001).